J Fluoresc (2008) 18:1059–1064
DOI 10.1007/s10895-008-0350-1

ORIGINAL PAPER

A Novel and Highly Sensitive Resonance Scattering Spectral Assay for Horseradish Peroxidase Using Cationic Surfactant

Ai-Hui Liang · Bo Jiang · Ji Ma · Zhi-Liang Jiang · Ji-Shun Li

Received: 24 November 2007 / Accepted: 7 February 2008 / Published online: 27 February 2008

Abstract A novel and ultrasensitive resonance scattering (RS) spectral assay was proposed for detection of horseradish peroxidase (HRP) activity. It was based on that the HRP strongly catalyze H_2O_2 oxidation of excess I^- to form I_3^-, the resulting I_3^- combined with four cationic surfactant (CS), including tetradecyl pyridinium bromide (TPB), cetyltrimethyl ammonium bromide (CTMA), cetylpyridinium chloride (CPCM) and tetradecyl dimethylbenzyl ammonium chloride (TDMBA) to produce association particles $(TPB\text{-}I_3)_n$, $(CTMA\text{-}I_3)_m$, $(CPCM\text{-}I_3)_l$ and $(TDMBA\text{-}I_3)_k$, which exhibit a strongest resonance scattering peak at 478, 423, 538 and 491 nm, respectively. For the four systems of TPB, CPCM, CTMBA and TDMBA, the HRP activity determined was in the linear range of 0.004–5.6, 0.04–3.2, 0.04–8.0, 0.08–8.0 ng/mL, with a detection limit of 0.0034, 0.040, 0.033, 0.016 ng/mL, respectively. The TPB resonance scattering spectral assay was best and has been applied to the analysis of HRP in real samples, with satisfactory results.

Keywords Horseradish peroxidase · Cationic surfactants · Association particles · Resonance scattering spectral assay

A.-H. Liang · B. Jiang · J. Ma · Z.-L. Jiang · J.-S. Li
Key Laboratory of New Processing Technology for Nonferrous Metals and Materials of Education Ministry,
Guilin University of Technology,
Guilin 541004, China

Z.-L. Jiang (✉)
Guangxi Key Laboratory of Environmental Engineering, Protection and Assessment, Guangxi Normal University,
Guilin 541004, China
e-mail: zljiang@mailbox.gxnu.edu.cn

Introduction

Horseradish peroxidase (HRP) is a very important enzyme with wide application in the fields of analytical chemistry, environmental science, clinical chemistry, organic synthesis and so on [1–6]. Based on the catalytic effect of HRP on H_2O_2 oxidation of some colorless aniline and phenols to dimmers and polymers of quinoid or azo type with color, fluorescence or electrochemical activity, it can not only be applied to detect the enzyme activity and H_2O_2 but also to enzymatic analysis and enzyme-linked immunoassay, with spectrophotometric, fluorophotometric and electrochemical techniques. Because of HRP being higher catalyzing efficiency, it can be used for treatment of the pollution caused by phenols and aromatic amines, and demonstrated abroad application prospect [1–2]. In addition to, HRP catalytic reaction has specificity, easy to controlling reaction, no by-products in poly-synthesis, and easy separation of its product, it has been paid attention to organic–synthetic chemists [5, 6].

At present, the main assays for detecting HRP activity include spectrophotometry, fluorescence spectrometry (FS), chemiluminescence method (CL), and ELISA, enzyme-linked fluorescence immunoassay, electrochemical enzyme-linked immunoassay. Among which, the voltammetric enzyme-linked immunoassay is of higher sensitivity but complicated to operate. Most substrates used in the assays above, aminobenzenes and phenols derivatives, are of unstability, easy to be oxidized when exposed to light or air, in addition, the carcinogenicity of aminobenzenes makes its application limited. Therefore, the study of new detection technique and new assays for the determination of HRP are of great significance. Light scattering is a commonly optical phenomenon. It was known that there are some electrons on the nanoparticle surface, in which

electrons located in the ground state or excited state. The energy between the ground state and the excitation state was called as excited energy. When the excited photon energy is same or close at the excited energy of the surface electrons, in which the excited photon resonate with the electron, that cause the scattering signal enhanced greatly. This optical phenomenon was called as resonance scattering (RS) effect or resonance light scattering effect. Based on the RS effect, a RS analytical technique has been developed to determine some inorganic and organic substances [7–16], with high sensitivity, good selectivity, simplicity and convenience. Recently, RS effect of inorganic nanopaticles has been applied to the analytical field [17, 18]. However, there are neither few reports on the study of RS effect of association particles, nor the detection of the activity of enzymes. In our present work, we have found that KI, which is of no toxicity and easy to be obtained, can act as a substrate for HRP, and the oxidation product of I_3^- combined with CS to form association particles, exhibiting RS effect. Based on those grounds, a novel, selective, sensitive and simple RS spectral assay has been proposed for the determination of ultratrace HRP.

Experimental section

Materials and reagents

A 5×10^{-8} g/mL HRP (biochemical reagent, RZ [$=A_{403\ nm}/A_{275\ nm}$] more than 3, 300 U/mg, Huamei Biological Engineering Co.) was prepared by dissolving 5.0 mg HRP to 10 mL with water was stored in −4 °C refrigerator and diluted gradually with double-distilled water to obtain the concentration required. 5.0×10^{-4} mol/L tetradecylpyridinium bromide (TPB), 1.0×10^{-4} mol/L cetyltrimethyl ammonium bromide (CTMBA), 5.0×10^{-4} mol/L cetylpyridinium chloride (CPCM), 1.0×10^{-4} mol/L tetradecyl dimethyl benzyl ammonium chloride (TDMBA) were purchased from Chemical Reagent Company of Medicine Group, Shang Hai, China. A 0.2 mol/L HAc, 0.2 mol/L NaAc, 0.06 mol/L KI, and 2.16×10^{-4} mol/L H_2O_2 were prepared. Diagnosis kit for hepatitis B virus surface antigen (HbsAg, enzyme-linked immunoassay, the batch number was 20050520) was purchased from Kehua Commercial Industrial & Biotechnology Co. Ltd, Shanghai. All the reagents were of analytical grade and all solutions were prepared in double-distilled water.

Apparatus

A model Cary Elips spectrofluorometer (Australia), a model TU-1910 double-beam UV-Vis spectrophotometer (Puxi General Instrumental Company, China), a model TDK temperature controller (Yujia Instrument Detecting Factory, China), and a model Nano-ZA90 nanoparticle size and potentiometric analyzer (Malvern Co., GB) were used.

Procedure

A NaAc–HAc buffer solution, 0.06 mol/L KI and 0.1 μg/mL HRP were piped into a 5.0 mL mark test tube, mixed well and incubated at 20 °C for 30 min, and CS was added, respectively. After mixing thoroughly, the RS spectra of the four systems were recorded on a spectraflorophotometer under the condition of that the excited wavelength λ_{ex} was equal to the emission wavelength λ_{em} ($\lambda_{ex}=\lambda_{em}$), the voltage was 400 V, the excited and emission slit width were both 5.0 nm. The RS intensity I_{RS} was recorded. A reagent blank (I_0) without HRP was recorded and the value of ΔI_{RS} ($=I_{RS}-I_0$) was also calculated.

Results and discussion

In the NAc–HAc buffer solution, the oxidation of KI by H_2O_2 to form I_3^- is quite slow, while the reaction becomes fast in the presence of HRP owing to it catalyzed H_2O_2 to yield OH. Then the resulting OH can oxidize excess I^- to form I_3^- that combined with CS and finally aggregate spontaneously to form $(CS\text{-}I_3)_n$ association particles. The laser scattering indicated the mean diameter of the association particles in the HRP–H_2O_2–KI–TPB system is 751 nm (Fig. 1). Thus, the system exhibits a RS effect, owing to formation of the association particles and the solid liquid interface. The main reactions are as following,

$$H_2O_2 \xrightarrow{\text{HRPCat.}} \cdot OH \quad (1)$$

$$\cdot OH + I^-(\text{Excess}) \longrightarrow OH^- + I_3^- \quad (2)$$

$$nCS^+ + nI_3^- \longrightarrow (CS - I_3)_n \quad (3)$$

We known that the reaction of Eqs. 2 and 3 was fast, the reaction of Eq. 1 was slow. According to reaction 1 and 2, the relationship between OH concentration (C_{OH}) and I_3^- concentration (C_I) was,

$$C_{OH}=k_{OH}C_I \quad (4)$$

According to reaction 3, the relationship between the $(CS\text{-}I_3)_n$ particle concentration (C_P) and I_3^- concentration (C_I) was,

$$C_P=k_P\,C_I \quad (5)$$

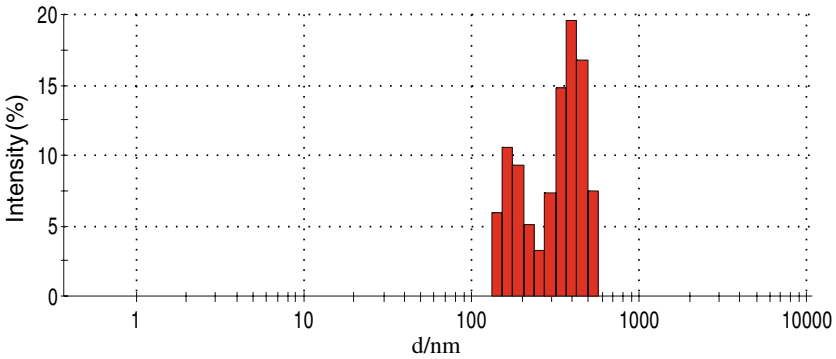

Fig. 1 Diameter distribution for the TPB system pH 4.6—4.0×10^{-5} mol/L TPB–0.24 ng/mL HRP–1.51×10^{-5} mol/L H_2O_2–4.8×10^{-3} mol/L KI

Based on the catalytic kinetic principle, the rate equation was written as,

$$\Delta C_P/\Delta t = k_K C_{HP}^{\alpha} C_{HRP} \quad (6)$$

Where C_{HP} and C_{HRP} are concentration of H_2O_2 and HRP, the k_{OH}, k_P and k_K are constant. According to the scattering equation of $I_{RS}=k_{RS}C_P$ (the k_{RS} is a constant) and above equation, the Eq. 6 can be rewritten as,

$$\Delta I_{RS}=\left(k_{RS}k_K k_P/k_{OH}C_{PO}{}^{\alpha}\Delta t\right)C_{HRP} \quad (7)$$

The Eq. 7 indicated that the ΔI_{RS} was linear to HRP concentration when other conditions hold constant.

RS and absorption spectra

Figure 2 shows the $(TPB\text{-}I_3)_n$ association particles exhibit a Rayleigh scattering peak at 478 nm. The studies of liquid phase inorganic nanoparticles indicate that three factors, including the light source of the apparatus, absorption of free molecule in the system and the RS effect of particles, causes synchronous scattering peak. The strongest emission of the apparatus is at 465 nm, so the system may exhibit a synchronous scattering peak at 465 nm. The absorption spectra (Fig. 3) indicated that I_3^- with low concentration and CS such as TPB exhibit very weak molecular absorption at the wavelength between 300 and 800 nm, so the effect caused by free molecules on the Rayleigh scattering spectra can be neglected. But the $(TPB\text{-}I_3)_n$ system has two absorption peaks. The laser scattering spectra revealed these two absorption peaks would have not appeared if there was no association particle exist, which demonstrated that the two peaks are surface plasma absorption peak of the $(TPB\text{-}I_3)_n$ particles [19], that is, this system had RS effect. Therefore, the peak at 478 nm was caused by the formation of association particles. There is no synchronous scattering peak at the 465 nm, owing to the RS effect being stronger. A wavelength of 478 nm for TPB system was chosen. The RS peaks for other three systems showed in the Table 1 and the wavelength at the strongest RS peak was used.

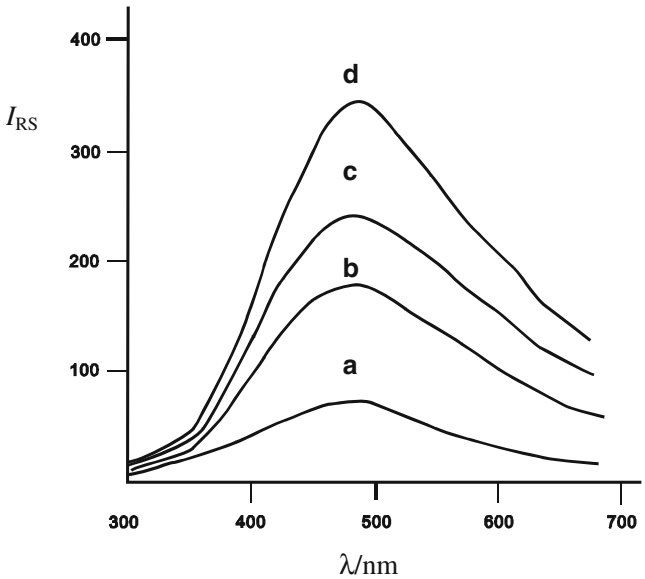

Fig. 2 RS spectra of the TPB system. *a* pH 4.6—4.80×10^{-3} mol/L KI–1.51×10^{-5} mol/L H_2O_2–4.0×10^{-5} mol/L TPB; *b a*—1.5 ng/mL HRP; *c a*—2.4 ng/mL HRP; *d a*—4.0 ng/mL

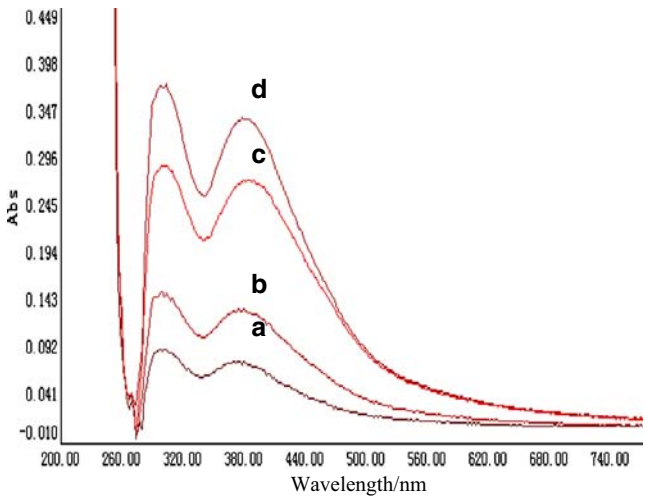

Fig. 3 Absorption spectra of the TPB system. *a* pH 4.6—4.80×10^{-3} mol/L KI–1.51×10^{-5} mol/L H_2O_2–4.00×10^{-5} mol/L TPB; *b a*—0.40 ng/mL HRP; *c a*—2.40 ng/mL HRP; *d a*—3.20 ng/mL HRP

Table 1 RS peaks for CS–HRP–H_2O_2–KI particle system

CS particle system	Color	RS peaks (from strongest to weaker; nm)
TPB	Light yellow	478 (strongest)
CTMAB	Light violet	423 (strongest), 270, 720
CPCM	Light yellow	538 (strongest), 400, 710, 270
TDMBA	Light yellow	491 (strongest), 390, 700, 270

Selection of conditions

Effect of pH

The effect of KH_2PO_4–Na_2HPO_4 buffer solution with the pH 4.9 to 8.04, HAc–NaAc in the pH 3.6 to 5.6 on the ΔI_{RS} values of the four systems were studied. The results showed the sensitivity of NaAc–HAc buffer solution is higher than KH_2PO_4–Na_2HPO_4. In the NaAc–HAc buffer solution, the ΔI_{RS} values of TPB, CTMAB and TDMBA systems reached their maximum and stable when the pH value is between 4.4 and 5.0 (Fig. 4). Thus, a pH 4.6 was chosen for the three systems. While ΔI_{RS} value of CPCM system increased from pH 3.5 to 4.5 at first, then keep stable from pH 4.5 to pH 5.5, thus pH 4.8 was selected for the CPCM system. When the volume of 0.20, 0.20, 0.20, and 0.30 mL for the TPB, CTMAB, CPCM and TDMBA systems, the ΔI_{RS} reached their maximum value, and was selected.

Effect of H_2O_2

As Fig. 5 shows the ΔI_{RS} value increased fast with the concentration of H_2O_2 when its concentration was low. The

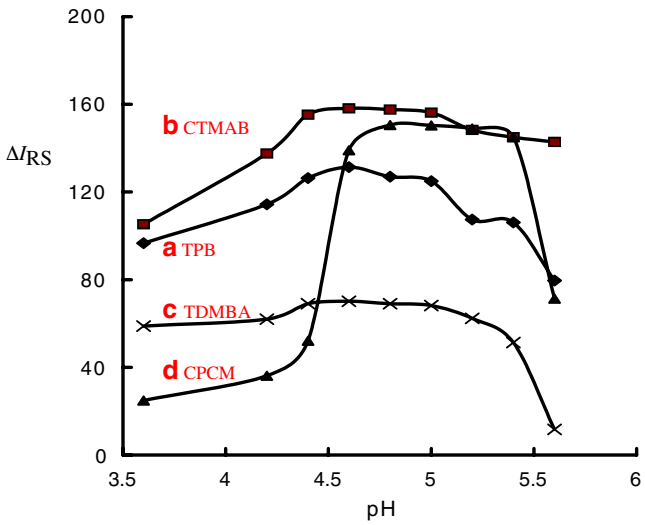

Fig. 4 Effect of pH. *a* TPB system; *b* CTMAB system; *c* CPCM system; *d* TDMBA system

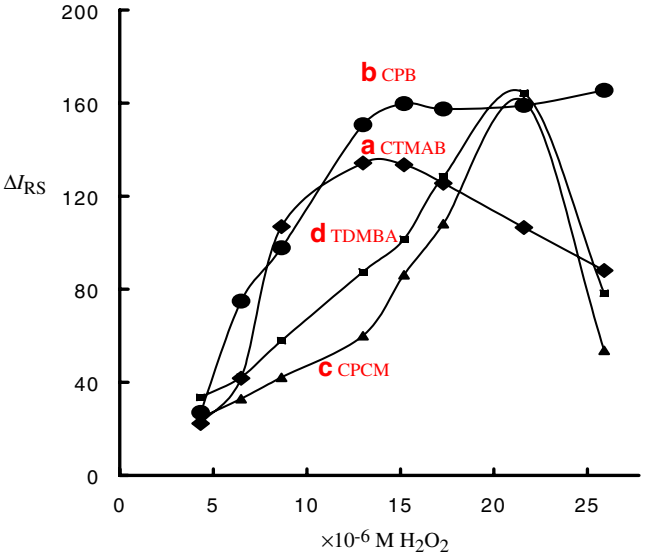

Fig. 5 Effect of H_2O_2 concentration. *a* CTMAB system; *b* TPB system; *c* CPCM system; *d* TDMBA system

ΔI_{RS} value of the TPB system tended to be stable when the concentration of H_2O_2 reached 1.51×10^{-5} mol/L. When the concentration of H_2O_2 was 1.31×10^{-5}, 2.16×10^{-5} and 2.16×10^{-5} mol/L for the system of CTMAB, CPCM and TDMBA, the ΔI_{RS} values all reached their maximum, then the ΔI_{RS} value gradually decreased as the concentration of H_2O_2 increased. So, 1.51×10^{-5} mol/L, 1.30×10^{-5} mol/L, 2.16×10^{-5} mol/L and 2.16×10^{-5} mol/L H_2O_2 were optimal for the TPB, CTMAB, CPCM and TDMBA systems, respectively.

Effect of KI

The ΔI_{RS} value of each system all increased quite fast as the concentration of KI increased when the KI at the very low concentration. When the concentration of KI reached 4.80×10^{-3} mol/L, 3.60×10^{-3} mol/L for TPB and CTMAB systems respectively, the ΔI_{RS} values reached their maximum and inclined to be stable. When the concentration of KI reached 6.00×10^{-3} mol/L, 7.20×10^{-3} mol/L for CPCM and TDMBA systems, respectively, the ΔI_{RS} values reached their maximum, too. Therefore, 4.80×10^{-3}, 3.60×10^{-3},

Table 2 Analytical features of CS systems

Systems	Regression equation	Linear range (ng/mL)	Correlation coefficient	Detection limit (ng/mL)
TPB	$\Delta I_{478\ nm}=55.6c+1.9$	0.004–5.60	0.9968	0.0034
CTMAB	$\Delta I_{423\ nm}=48.2c+0.37$	0.040–3.20	0.9982	0.040
CPCM	$\Delta I_{538\ nm}=57.7c-10.7$	0.040–8.0	0.9955	0.033
TDMBA	$\Delta I_{491\ nm}=10.2c+20.1$	0.080–8.0	0.9958	0.016

Table 3 Influence of FS

FS	Allowance C_{FS}/C_{HRP}	RE (%)	FS	Allowance C_{FS}/C_{HRP}	RE (%)
BSA	2.5×10^{3}	1.4	HSA	5.5×10^{2}	8.8
b-Amylase	1.2×10^{3}	7.7	Sucrose	8.3×10^{3}	5.3
L-Aspartate	3.3×10^{3}	0.8	V_B6	8.3×10^{4}	3.7
DL-Tryptophan	1.3×10^{2}	−5.3	Mg^{2+}	3.3×10^{3}	6.9
Glycine	6.7×10^{3}	3.6	Ca^{2+}	1.2×10^{4}	1.4
L-Glutamate	1.5×10^{4}	1.9	K^{+}	1.3×10^{5}	5.7
Nicotinicaid	5.0×10^{3}	7.5	Cu^{2+}	1.7×10^{3}	−5.8
SO_4^{2-}	1.3×10^{5}	6.9	Zn^{2+}	3.3×10^{3}	8.9
$C_2O_4^{2-}$	1.1×10^{5}	2.0	Fe^{3+}	3.3×10^{2}	−3.0
Cl^{-}	1.8×10^{5}	5.7	Ni^{2+}	2.3×10^{2}	5.0
Citric acid	4.6×10^{5}	8.4	SDS	1.0×10^{2}	−5.4

6.00×10^{-3} and 7.20×10^{-3} mol/L KI were chosen for the TPB, CTMAB, CPCM and TDMBA systems, respectively.

Effect of CS

When the concentration of TPB, CTMAB, CPCM and TDMBA was 3.0×10^{-5}, 1.5×10^{-5}, 6.0×10^{-5} and 1.0×10^{-5} mol/L for each system, the ΔI_{RS} values reached their maximum and became stable. Therefore, 4.0×10^{-5} mol/L TPB, 2.0×10^{-5} mol/L CTMAB, 8.0×10^{-5} mol/L CPCM and 1.2×10^{-5} mol/L TDMBA were chosen for use.

Effect of reaction time and temperature

The results indicated, at the temperature between 18 to 25 °C, the ΔI_{RS} value is maximum and relatively stable and the HRP activity was high. At the temperature of 37 °C, the activity of HRP was quite high, however, the blank value was also high and the ΔI_{RS} was unstable. The ΔI_{RS} values all reached their maximum, needing about 25 min, kept stable within 50 min. Thus, reaction time of 30 min at 20 °C was chosen for each system.

Working curve

The working curves were obtained by measuring the ΔI_{RS} for each system by adding RP of various concentrations. Table 2 shows the ΔI_{RS} value is proportional to the HRP concentration in a certain range, in which the TPB system was relatively sensitive and reproducible. Thus, the TPB system was chosen for the analysis of samples. Compared with those methods already reported [20–25], the one described in this paper has some advantages, including the reagents of no carcinogenicity and easy to be obtained, and high sensitivity, so it is one of the most sensitive assays for the determination of HRP activity.

Influence of Foreign Substances

The influence of foreign substances (FS) on the determination of 2.40×10^{-2} ng/mL HRP was examined. When the relative error (RE) is less than ±10%, the tolerances of coexisting substances are showed in Table 3. It can be seen that most of constant substances examined didn't interfere with the determination of HRP. The results indicated that the present method has good selectivity.

Analysis of Samples and Recovery

The HRP concentrations in real samples of the HbsAg were detected under the optimum conditions and the results are listed in Table 4. The relative standard deviation (RSD) was between 4.6% and 7.7%. The recovery was in the range of 101% to 110.0%.

Conclusions

A novel and ultrasensitive and highly selective RS assay was proposed for the determination of HRP, combined the RS effect of $(CS\text{-}I_3)_n$ particle and the strong catalytic effect of HRP. It would be widely applied to enzyme-linked

Table 4 Results for HRP in samples

Sample	Found value (mg/mL)	Average (μg/mL)	RSD (%)	Added (ng/mL)	Found (ng/mL)	Recovery (%)
1	1.20, 1.12, 1.17, 1.08, 1.10	1.14±0.053	4.6	1.0	1.02	102
2	0.129, 0.125, 0.139, 0.134, 0.118	0.132±0.0081	6.1	0.1	0.103	103
3	0.0152, 0.0143, 0.0126, 0.0151, 0.0136	0.0143±0.0011	7.7	0.01	0.0107	107

immunoassay, coupling this new strategy with the enzyme labeled immuoreaction.

Acknowledgement This work was supported by the Foundation of New Century Ten-Hundred-Thousand Talents of Guangxi and the Research Funds of Guangxi Key Laboratory of Environmental Engineering, Protection and Assessment, and the Foundation of Guilin University of Technology.

References

1. Huang QI, Selig HI, Walter J, Weber JR (2002) Peroxidase-catalyzed oxidative coupling of phenols in the presence of geosorbents: rates of non-extratable product formation. Environ Sci Technol 36:596–6202
2. Huang Q, Weber WJ (2005) Transformation and removal of bisphenol A from aqueous phasevia peroxidase mediated oxidative coupling reactions: efficacy, products, and pathways. Environ Sci Technol 39:6029–6036
3. Jiao K, Sun W, Zhang SS (2000) Comparison of electrochemincal and spectrophotometric detection in HRP-based ELISA fortobacco mosaic virus. Anal Lett 33:2653–2675
4. Yao H, Li N, Xu S, Xu JZ, Zhu JJ, Chen HY (2005) Electrochemical study of a new methylene blue/silicon oxide nanocomposition mediator and its application for stable biosensor of hydrogen peroxide. Biosens Bioelectron 21:372–377
5. Pablo FB, Mar'ıa BGG, Agust'ın CG (2004) Voltammetric determination of alkaline phosphatase and horseradish peroxidase activity using 3-indoxyl phosphate as substrate Application to enzyme immunoassay.. Talanta 64:452–457
6. Jin Z, Su YX, Duan YX (2001) Anovel method for polyaniline synthesis with the immobilized horseradish peroxidase enzyme. Synth Met 122:237–242
7. Alva KS, Lee TS, Kumar J (1998) Enzymatically synthesized photodynamic polyaniline containing azobenzene groups. Chem Mater 10:1270–1275
8. Wu LP, Li YF, Huang CZ, Zhang Q (2006) Visual detection of Sudan dyes based on the plasmon resonance light scattering signals of silver nanoparticles. Anal Chem 78:5570–5577
9. Liu SP, Luo HQ, Li NB, Liu ZF (2001) Resonance Rayleigh scattering study of the interaction of heparin with some basic diphenyl napthylmethane dyes. Anal Chem 73:3907–3914
10. Luo HQ, Li NB, Liu SPu (2006) Resonance Rayleigh scattering study of interaction of hyaluronic acid with ethyl violet dye and its analytical application. Biosens Bioelectron 21:1186–1194
11. Guo CX, Shen HX (2000) Sensitive and simple determination of protein by resonance Rayleigh scattering with 4-azochromotropic acid phenylfluorone. Anal Chin Acta 408:177–182
12. Han ZQ, Qi L, Shen GY, Liu Wi, Chen Y (2007) Determination of hromium(VI) by surface plasmon field-enhanced resonance light scattering. Anal Chem 79:5862–5868
13. Pan HC, Liang FP, Mao CJ, Zhu JJ, Chen HY (2007) Highly luminescent zinc(II)-bis(8-hydroxyquinoline) complex nanorods: sonochemical synthesis, characterizations, and protein sensing. J Phys Chem B 111:5767–5772
14. Du BA, Li ZP (2006) One-step homogeneous detection of DNA hybridization with gold nanoparticle probes by using a linear light-scattering technique. Angew Chem Int Ed 45:8022–8025
15. Jiang ZL, Sun SJ, Liang AH, Huang WX, Qin AM (2006) Gold-labeled nanoparticle-based immunoresonance scattering spectral assay for trace apolipoprotein AI and apolipoprotein B. Clin Chem 52:1389–1394
16. Jiang ZL, Zhou SM, Liang AH, Kang CY, He XC (2006) Resonance scattering effect of rhodamine dye association nanoparticles and its application to respective determination of trace ClO_2 and Cl_2. Environ Sci Technol 40:4286–4291
17. Liang AH, Jiang ZL, Zhang BM, Liu QY, Lu X (2005) A new resonance scattering spectral method for the determination of trace amounts of iodate with rhodamine 6G. Anal Chim Acta 530:130–134
18. Hou M, Sun SJ, Jiang ZL (2007) A new and selective and sensitive nanogold-labeled immunoresoance scattering spectral assay for trace prealbumin. Talanta 72:463–467
19. Park JE, Momma T, Osaka T (2007) Spectroelectrochemical phenomena on surface plasmon resonance of Au nanoparticles immobilized on transparent electrode. Electrochim Acta 52:5914–5923
20. Siddiqi IW (1982) An electrochemical assay system for peroxidase and peroxidase-coupled reactions based on fluoride ion-selective electrode. Clin Chem 28:1962–1967
21. Molaei Rad A, Ghourchian H, Moosavi-Movahedi AA, Hong J, Nazari K (2007) Spectrophotometric assay for horseradish peroxidase activity based on pyrocatechol–aniline coupling hydrogen donor. Anal Biochem 362:38–43
22. Wei YF, Yan HT (2001) Catalytic spectrophotometric determination of horseradish peroxidase. Guang Pu Xue Yu Guang Pu Fen Xi 21:704–706
23. Wei YF, Yan HT (2000) Catalytic spectrofluoremetric determination of horseradish peroxidase. Chin J Anal Chem 28:99–101
24. Zhang SS, Jiao K, Chen HY, Li HJ (1999) Spectral and electrochemical study of MAP–H_2O_2–HRP voltammetric enzymatic-immunoassay system. Acta Chim Sin 57:922–930
25. Suna W, Jiao K, Zhang SS, Zhang CL, Zhang ZF (2001) Electrochemical detection for horseradish peroxidase-based enzyme immunoassay using *p*-aminophenol as substrate and its application in detection of plant virus. Anal Chim Acta 434:43–50